RD Status Report/RD39
18th February 2010

RD39 STATUS REPORT 2009

CERN RD39 Collaboration

P. Anbinderis[m], T. Anbinderis[m], R. Bates[e], W. de Boer[h], E. Borchi[c], M. Bruzzi[c], S. Buontempo[k], C. Buttar[e], W. Chen[b], V. Cindro[i], V. Eremin[l], E. Gaubas[m], J. Härkönen[g], E. Heijne[a], I. Ilyashenko[l], V. Kalesinskas[m], M. Krause[h], Z. Li[b], P. Luukka[g], I. Mandic[j], D. Menichelli[c], M. Mikuz[j], H. Moilanen[g], S. Mueller[h], T. Mäenpää[g],T.O. Niinikoski[a],V. O'Shea[e], S. Pagano[k], C. Parkes[e], S. Pirollo[c], P. Pusa[f] J. Räisänen[f], L. Spiegel[i], E. Tuominen[g], E. Tuovinen[g], J. Vaitkus[m], E. Verbitskaya[l], S. Väyrynen[f], M. Zavrtanik[i]

[a]*CERN, CH-1211 Geneva, Switzerland*
[b]*Brookhaven National Laboratory, Upton, NY 11973-5000, USA*
[c]*Dipartimento di Energetica, Universitá di Firenze, I-50139 Firenze, Italy*
[e]*Department of Physics and Astronomy, University of Glasgow, Glasgow G12 8QQ, United Kingdom*
[f]*Accelerator Laboratory, University of Helsinki, 00014 University of Helsinki, Finland*
[g]*Helsinki Institute of Physics, 00014 University of Helsinki, Finland*
[h]*IEKP University of Karlsruhe, D-76128 Karlsruhe, Germany*
[i]*Jozef Stefan Institute, Experimental Particle Physics Department, 1001 Ljubljana, Slovenia*
[j]*Fermi National Accelerator Laboratory, Batavia, IL 60510-501, USA.*
[l]*Ioffe Physico-Technical Institute, Russian Academy of Sciences, St.Petersburg 194021, Russia*
[m]*University of Vilnius, Institute of Materials Science and Applied Research, 2040 Vilnius, Lithuania*

CERN-LHCC-2010-004 / LHCC-SR-002
24/02/2010

Summary

CERN RD39 Collaboration is developing super-radiation hard cryogenic silicon detectors for applications of LHC experiments and their future upgrades. Radiation hardness up to 1×10^{16} n_{eq}/cm^2 will be required in the future HEP experiments. The most important measure of the detector's radiation hardness is the Charge Collection Efficiency (CCE), which is affected by the sensitive volume of the detector (depletion depth) and the charge trapping into the radiation-induced trapping centers. However, 1×10^{16} n_{eq}/cm^2 fluence is well beyond the radiation tolerance of even the most advanced semiconductor detectors fabricated by commonly adopted technologies. First, at this fluence the needed full depletion voltage (V_{fd}) would be in the scale of thousands of volts for a 300 μm thick Si detector operated at or near room temperature. Second, the charge carrier trapping will limit the charge collection depth to an effective range of 20 μm to 30 μm regardless of the depletion depth. In order to maintain an acceptable CCE in the Super-LHC radiation environment, one has to solve both problems simultaneously.

The activities of the RD39 Collaboration were focused in 2009 on the concept of a charge injected detector (CID). In a CID, the electric field is controlled by injected current, which is limited by the space charge. This leads to a continuous electric field through the detector at any operating voltage regardless of the radiation fluence. The electric field distribution in a CID is proportional to the square root of the distance starting from the charge injection contact. According to the calculations with known electric field distribution one could expect more than two times higher CCE in CID compared to a similar detector under reverse bias. Low temperature (-50°C) and a high concentration of deep levels are required in order to establish the stable electric field favorable for detector operation by charge injection. .

In 2009, two heavily irradiated full size CID detectors with 768 channels were tested in a beam at CERN H2 area. The p and n-type sensors were irradiated to the fluences of 2×10^{15} n_{eq}/cm^2 and 5×10^{15} n_{eq}/cm^2 , respectively and measured with CMS Tracker readout electronics (APV25). Our results indicate relative CCE of more than 30% for both devices with signal to noise ratios (S/N) of about 10 and 8 for 2×10^{15} n_{eq}/cm^2 and 5×10^{15} n_{eq}/cm^2 , respectively. The signal from the detector irradiated with 5×10^{15} n_{eq}/cm^2 could not be distinguished from the noise when the detector was reverse biased. In the detector irradiated with the fluence of 2×10^{15} n_{eq}/cm^2 the same CCE required twice as large bias voltage in the reverse bias mode as in the CID operation mode (500V). The test beam measurements were performed at -50^0C, which was obtained with a Peltier-element cooling system. However, this kind of temperature is also achievable by the carbon dioxide based cooling systems currently under investigation in the large experiments.

1. Introduction

For LHC upgrade, the Super-LHC, the expected radiation level will be 10 times higher, up to 1x10^{16} n_{eq}/cm^2 (n_{eq} stands for 1 MeV neutron equivalent fluence) than in the current LHC. About 90% of silicon sensors to be implemented in future trackeing systems are strip detector devices, which will accumulate fluence of 1×10^{15} n_{eq}/cm^2 or less. This radiation hardness target can be met by implementing standard p^+ on n-type doped silicon substrate (p on n detector structure) with advanced substrate technology such as Magnetic Czochralski silicon (MCz-Si) [1]. The Charge Collection Efficiency (CCE) will, however, degrade soon after the fluence of 1×10^{15} n_{eq}/cm^2 resulting in the sensors becoming unusable for particle tracking. The loss of CCE is due to both increase in trapping and collapse of the electric field.

It can be derived that for an MIP (minimum ionizing particle) detection in a pad detector with a constant weighting field [2,3] of 1/*d* (*d* being the detector thickness) and a constant electric field in the depletion depth of *w*, the total collected charge Q_c can be expressed as the following:

$$Q_c = Q_0 \frac{w}{d} \cdot \left(\frac{\tau_t^e}{t_{dr}^e}\left[1-\exp\left(-t_{dr}^e/\tau_t^e\right)\right] + \frac{\tau_t^h}{t_{dr}^h}\left[1-\exp\left(-t_{dr}^h/\tau_t^h\right)\right] \right) \qquad (1)$$

where Q_0 is the total charge deposited in the detector with a thickness of *d*, and Q_0 = 80 e's/μm ×*d* for MIP, t_{dr} is charge collection (drift) time, and τ_t is the trapping time constant, with notion of *e* for electrons and *h* for holes, respectively. For the non-fully depleted Si detectors, only the fraction *w/d* of the total deposited charge Q_0, which is generated by a MIP uniformly in the entire detector, contributes to the charge signal, whereas the rest is lost completely. At the S-LHC radiation fluences, the trapping time is very short, which means that $t_{dr}/\tau_t >> 1$, Eq. (1) can be reduced to:

$$Q_c \simeq 80\, e's/\mu m \cdot (v_{dr}^e \cdot \tau_t^e + v_{dr}^h \cdot \tau_t^h) \equiv 80\, e's/\mu m \cdot (d_t^e + d_t^h) \qquad (2)$$

where d_t^e and d_t^h are trapping distances for electrons and holes, respectively. It is clear that the collected charge at the S-LHC radiation fluences has no apparent dependence on the detector thickness and depletion depth as long as they are much larger than the trapping distances that are in the order of 20 μm at the fluence of 1x10^{16} n_{eq}/cm^2 for standard detectors and detector operations.

To improve the collected charge in the S-LHC environment, it is clear that one has to increase the trapping time for the carries since one can only increase the carrier drift velocity to the saturation values at high electric fields, i.e. $v_{dr}^{e,h} \le v_s^{e,h} \le 1\times10^7\, cm/s$. The carrier trapping time is related to the concentration of the empty traps $N_{t,empty}$ as the following:

$$\tau_t = \frac{1}{\sigma v_{th} N_{t,empty}} \qquad (3)$$

Where σ is the carrier capture cross section, and v_{th} is the carrier thermal velocity. Apparently, one needs to reduce the concentration of the empty traps. One way of doing that is to fill the traps by carriers injected through the contacts via external light (laser, LED, etc.) another via forward biasing.

The approach of the RD39 collaboration is to inject electrons through the n^+ contact in a Si detector by forward biasing the $p^+/n/n^+$ detector that has been irradiated beyond the space-charge-sign-inversion (SCSI). In such a detector the main junction is located near the n^+ contact. By injecting electrons with a substantial current, one can reach a dynamic equilibrium between the trapping and detrapping at a given temperature, in which most of the electron traps are filled up, and therefore no longer active in trapping the free electrons generated by the passing particles. Under these conditions, the electric field extends through the entire detector thickness regardless of the applied voltage or the concentration of the deep levels. Depending on the point of the injection, the electric field increases towards the back plane of the detector or vice versa. The amplitude of the electric field is proportional to the square root of the distance from the injecting junction. A schematic illustration of the difference between the electric field distribution in a heavily irradiated standard reverse biased detector and a charge injected detector is show in figure 1.

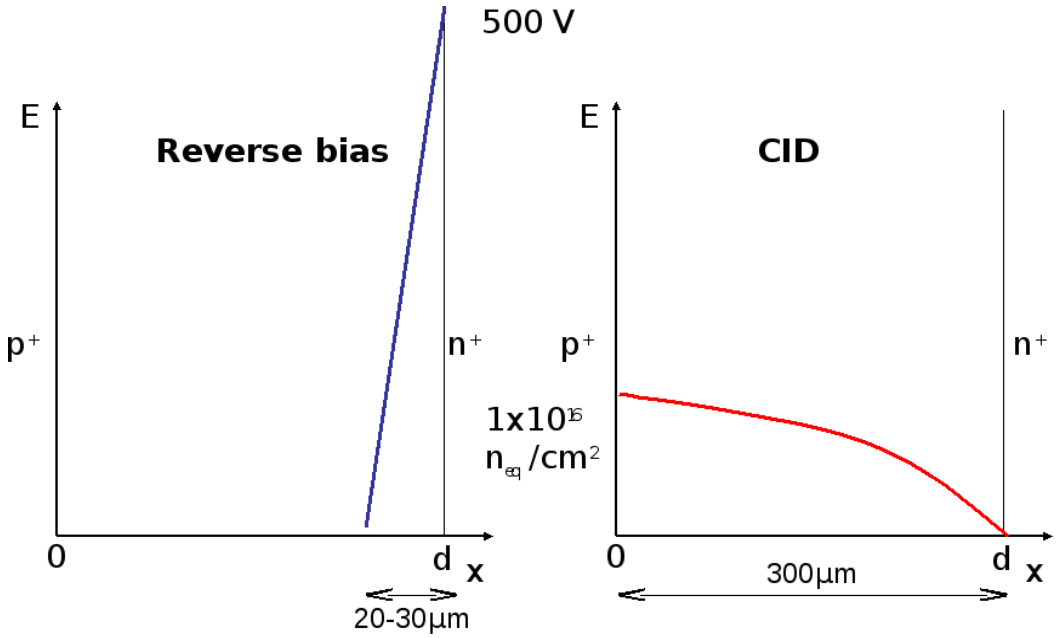

Figure 1. Illustration of the electric field distribution E(x) in a reverse biased and in a CID detector. .

1.1Temperature and forward current required for CID operation.

It is obvious that tracker systems operating in harsh radiation environments require cooling in order to remove the excess heat induced by the readout electronics and to suppress the shot noise caused by the leakage current due to the radiation defects. This is the case regardless whether the sensors are intended to be operated under reverse bias or CID mode. If the charge injection is realized by forward biasing the pn-junction, the current needed is determined by the balance between the trapping and its counter process detrapping, i.e. emission of the trapped charge carrier back into the signal transportation. The time constants of these competitive processes are given by

(4)

$$\tau_{trapping} = \frac{1}{\sigma_{e,h} v_{th} N_t}$$

$$\tau_{detrapping} = \frac{1}{\sigma_{e,h} v_{th} e^{\frac{-E_t}{kT}}}$$

where τ_d is the time constant for trapping, τ_d is the time constant for detrapping, σ is the capture cross section of the trap, v_{th} is the thermal velocity of the charge carriers, N_T is the concentration of the traps, N_C the electric state density in the conduction band, and E_t the trap energy level in the band gap. It can be seen that the trapping does not depend on the temperature, while the detrapping contains an exponential temperature dependence. This means that the amount of the forward current needed for an efficient charge injection is decreased rapidly with a decreasing temperature. On the other hand, under the harsh radiation environment the trapping is a limiting factor of the charge collection. Thus, the charge transportation must be as fast as possible in order to avoid loosing the particle generated charge into the radiation defects by trapping. This in turn, requires relatively high bias voltage in order to maintain a sufficient drift velocity through the thickness of the detector's sensitive volume.

$$v_{drift} = \mu_{e,h} E(x) \quad , \qquad (5)$$

where $\mu_{e,h}$ is the mobility of the electrons and holes, respectively. The equations (4) and (5) imply e.g. that CID cannot operate at the room temperature as a particle detector. At the room temperature, very high forward current would be required to fill the defects since the trapped charge would almost immediately be emitted back to the current transportation by the detrapping process. As a result, very small voltage would be required to inject this current and charge carriers would drift with very small velocity. For the same reasons, an non-irradiated silicon detector cannot operate as CID, not even at a low temperature. In the non-irradiated detector the concentration of the deep levels is usually negligible. Thus, all the deep levels would be filled with a very small current injection, which resulted in an insufficiently small electric field for an efficient charge drift. In practice, CID would require a S-LHC irradiation fluence, i.e. > 1×10^{15} n_{eq}/cm^2

for its operation. This is illustrated in figure 2., which shows simulated and measured IV characteristics of the CID detectors.

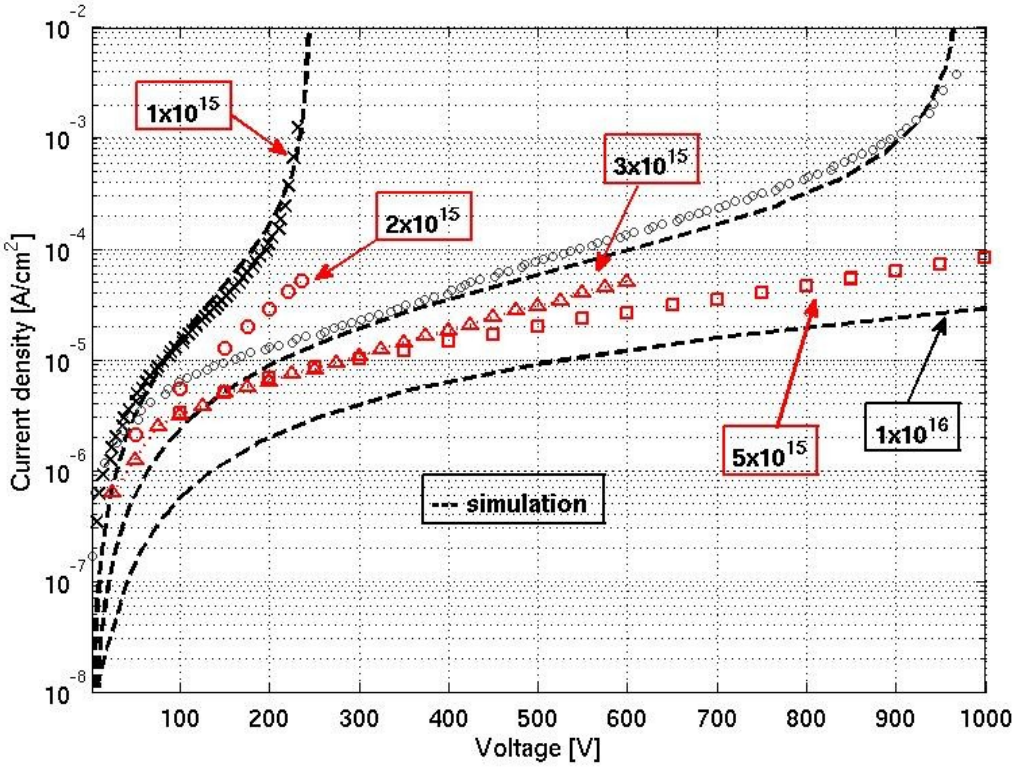

Figure 2. IV characteristics of CID detectors. The red open symbols (o Δ) correspond to strip detectors with 768 channels. The black dashed lines (---) are for simulations of the current and symbol (×) stands for a measurement of a diode. The measurements have been carried out at -50^{0}C temperature. The current values indicated for the strip detectors are recorded from the CAEN power supply biasing the detector module with APV25 readout.

As it can be seen in figure 2., for example a current density of 10 μA/cm^2 is reached at about 70V after 1×10^{15} n_{eq}/cm^2 and at about 150V after 2×10^{15} n_{eq}/cm^2 . After 3×10^{15} n_{eq}/cm^2 irradiation it takes more than 900V to reach the treshold (V_T) of abrupt current increase [4]. Respectively, if the CID detector is biased with constant voltage e.g. 200V, which provides the same electric field distribution regardless of the irradiation fluence, the forward current density decreases from about 100μA/cm^2 at 1×10^{15} n_{eq}/cm^2 to 2μA/cm^2 at 1×10^{16} n_{eq}/cm^2 .

2.Test beam measurements on CID detectors in 2009.

In 2009 two different CID strip sensors were characterized in a test beam at CERN H2 area using the Silicon Beam Telescope (SiBT) [5]. The SiBT is a telescope that accurately measures reference tracks of particles. The read-out electronics and data

acquisition (DAQ) system of SiBT consist of the CMS Tracker hybrids with APV25 chips and the CMS Tracker data acquisition cards. The telescope consists of eight reference detector planes and of two slots for the detectors to be tested. The test beam experiment and related data analysis was done as a common effort of FNAL, Helsinki, Brown, Karlsruhe and Rochester.

The n and p-type (p^+ strip implant on n-type wafer and n^+ strip implant on p-type wafer) detectors were processed at the Micronova Centre for Micro- and Nanotechnology of Helsinki University of Technology. The starting material of the detectors was 100 mm diameter double-side-polished 300±2 μm-thick <100> n and p-type Magnetic Czochralski silicon (MCz-Si) wafers. The nominal resistivity, measured by the four point probe method, of the wafers was 900-1100 Ωcm for n-type wafers and 3kΩcm for p-type wafers, respectively. The size of the strip detectors was 4cm × 4cm and there were 768 10 μm wide strips with a 50μm pitch [6].

The p and n-type sensors were irradiated to the fluences of 2×10^{15} n_{eq}/cm^2 and 5×10^{15} n_{eq}/cm^2, respectively, by 26 MeV protons at Karlsruhe. After the irradiations the detectors were wire bonded to the CMS APV25 hybrids via a pitch adapter at the CERN bonding laboratory. An overview of a CID module is shown in figure 3.

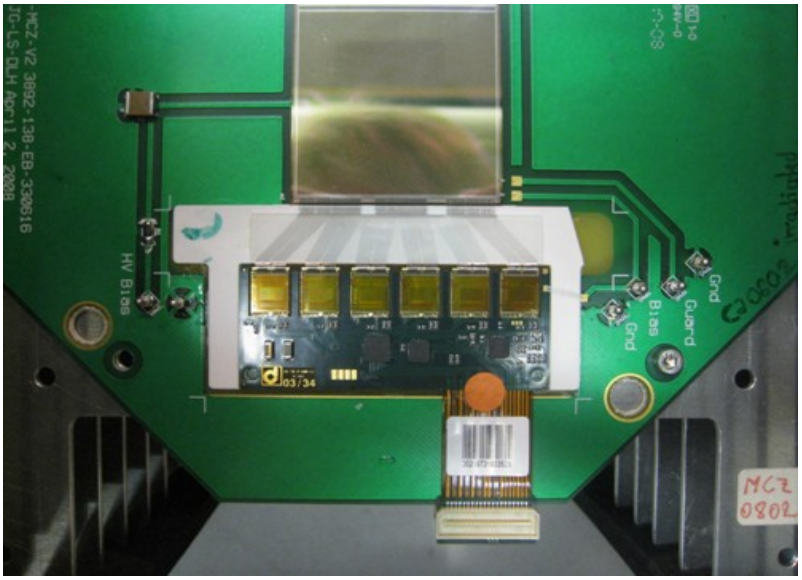

Figure 3. 768 channels 4cm × 4cm strip detector attached to the CMS readout module.

During the operation, the CID modules were placed into an external single-detector Peltier cooled cold box next to the SiBT telescope. The experimental arrangement is shown in our previous status reports figure 9 [7]. In the following plots, the temperature of the cold finger of the separate cold box was -53^0C unless otherwise stated.

Figure 4. shows the collected charge of a 5×10^{15} n_{eq}/cm^2 irradiated $p^+/n^-/n^+$ CID detector as a function of bias.

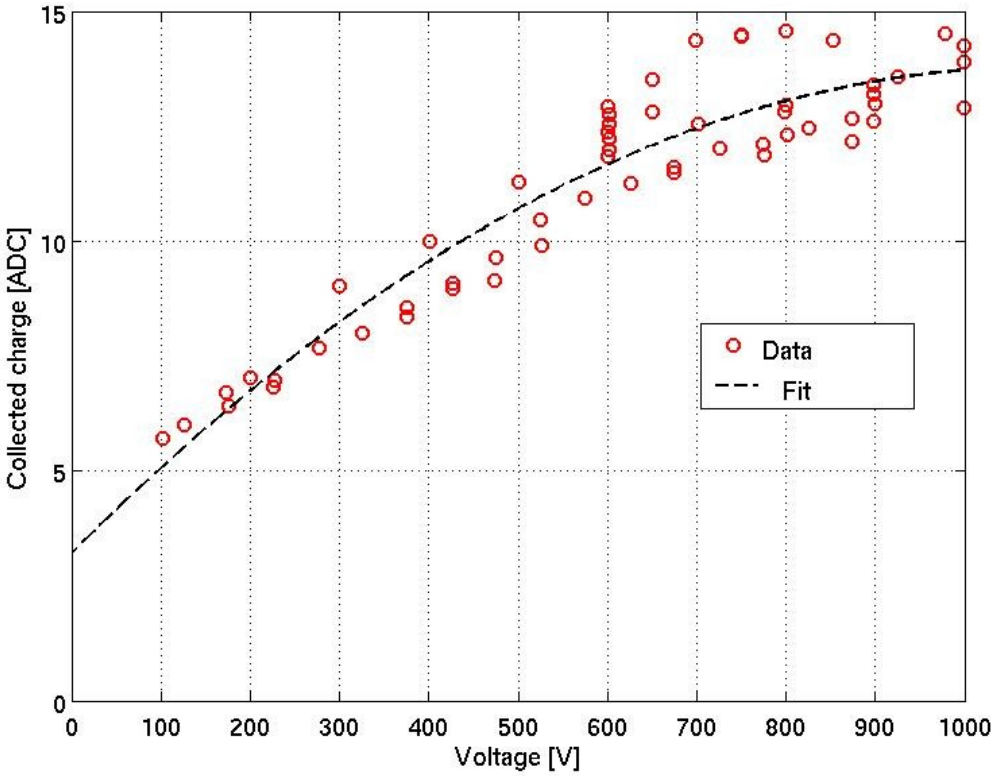

Figure 4. Collected charge of the 5×10^{15} n_{eq}/cm^2 irradiated $p^+/n^-/n^+$ CID detector. As a reference, the full charge recorded from the non-irradiated reference planes is approximately 40 ADC counts.

As discussed in chapter 1.1. and reference [4], it was possible to bias 5×10^{15} n_{eq}/cm^2 irradiated module up to 1000V before the abrupt current increase after space charge saturation took place. The forward current of the module at 1000V was 440μA and 110μA at 600V bias. The collected charge at 1000V is about 14.4, which is an average of three runs with about 3200 analyzed events. As it can be seen in figure 4, at 600V there are eight data points. The average ADC value of these data points is 12.4 with more than 10 000 events. As reported in references [1,8], the full charge recorded from the non-irradiated reference planes is approximately 40 ADC counts. Thus, the relative CCE of the 5×10^{15} n_{eq}/cm^2 irradiated CID detector at 600V was about 31% and 36% at 1000V. The Landau-distribution of the charge measurements at 600V with respect to a non-irradiated reference is shown in figure 5.

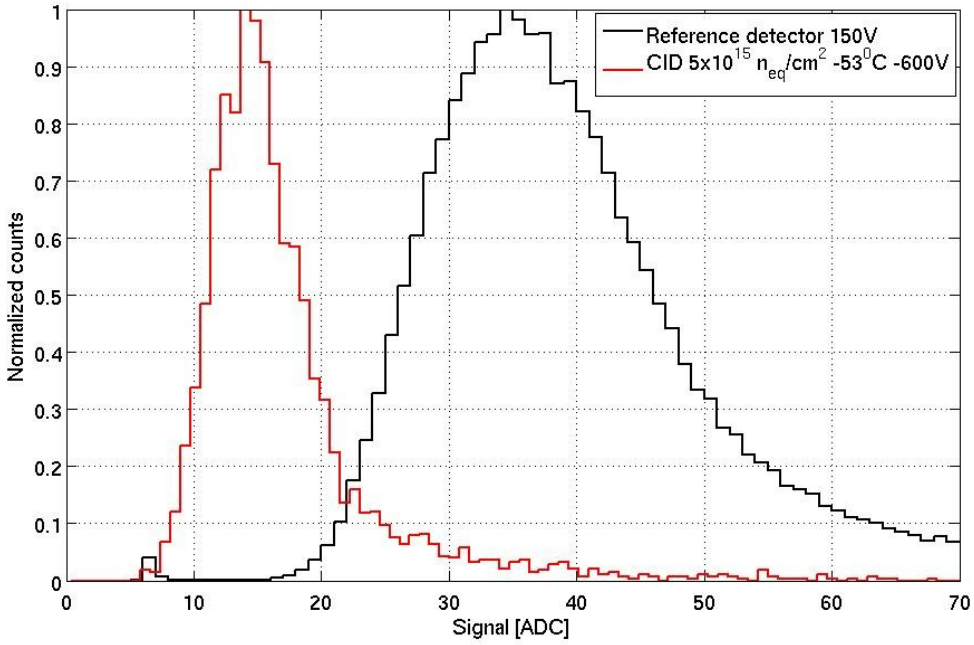

Figure 5. Landau distribution of charge measurements of 5×10^{15} n_{eq}/cm^2 irradiated CID detector at 600V. The data for this plot has been taken from different runs with different amount of data. The signal distribution for CID detector consists of 3255 events and the distribution for reference consists of 6615 counts.

Figure 6. illustrates the noise recorded from 5×10^{15} n_{eq}/cm^2 irradiated CID detector at 600V.

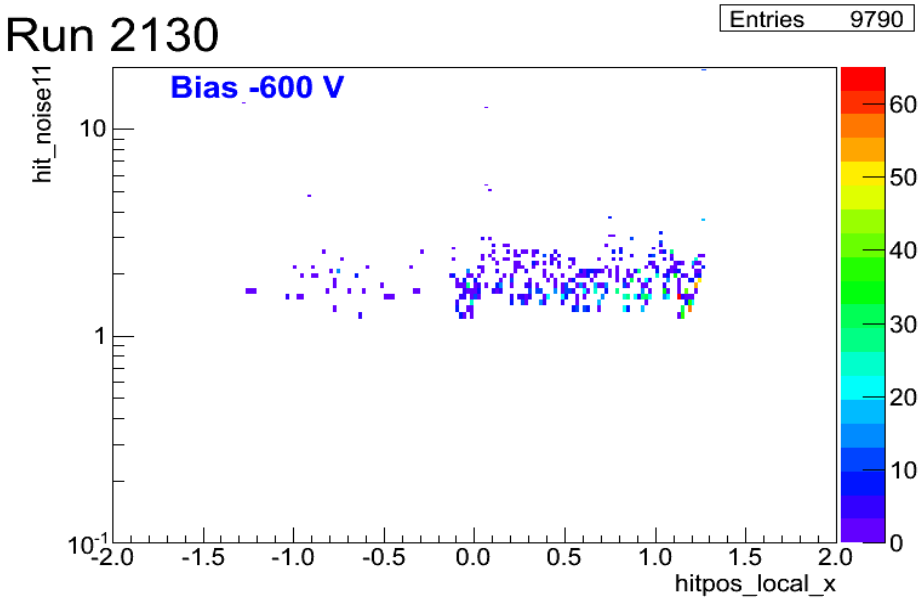

Figure 6. The noise recorded from 5×10^{15} n_{eq}/cm^2 irradiated CID detector at 600V bias.

The mean value of the noise shown in figure 6 is about 1.6 ADC. Thus, the signal-to-noise ratio (S/N) of the 5×10^{15} n_{eq}/cm^2 irradiated CID detector at 600V bias is about 8.

Another detector investigated by the RD39 Collaboration during the 2009 test beam campaign was $n^+/p^-/p^+$ structure strip sensor processed on p-type MCz-Si substrate and irradiated with 26 MeV protons to 2×10^{15} n_{eq}/cm^2 effective fluence. With such relatively low fluence, the threshold voltage for space charge saturation (V_T) followed by sharp current increase took place after 200V forward bias. Figure 7 shows the collected charge as a function of bias voltage.

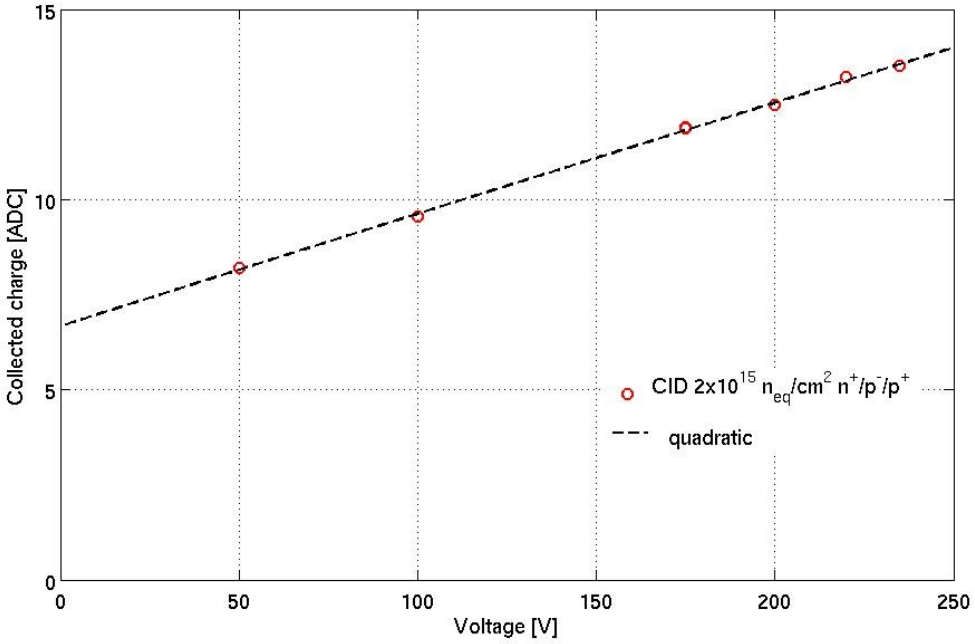

Figure 7. Collected charge of a 2×10^{15} n_{eq}/cm^2 irradiated $n^+/p^-/p^+$ CID detector.

The highest collected charge of this module was obtained at 230V and corresponds to about 13.5 ADC counts. The noise as a function of bias voltage is shown in figure 8.

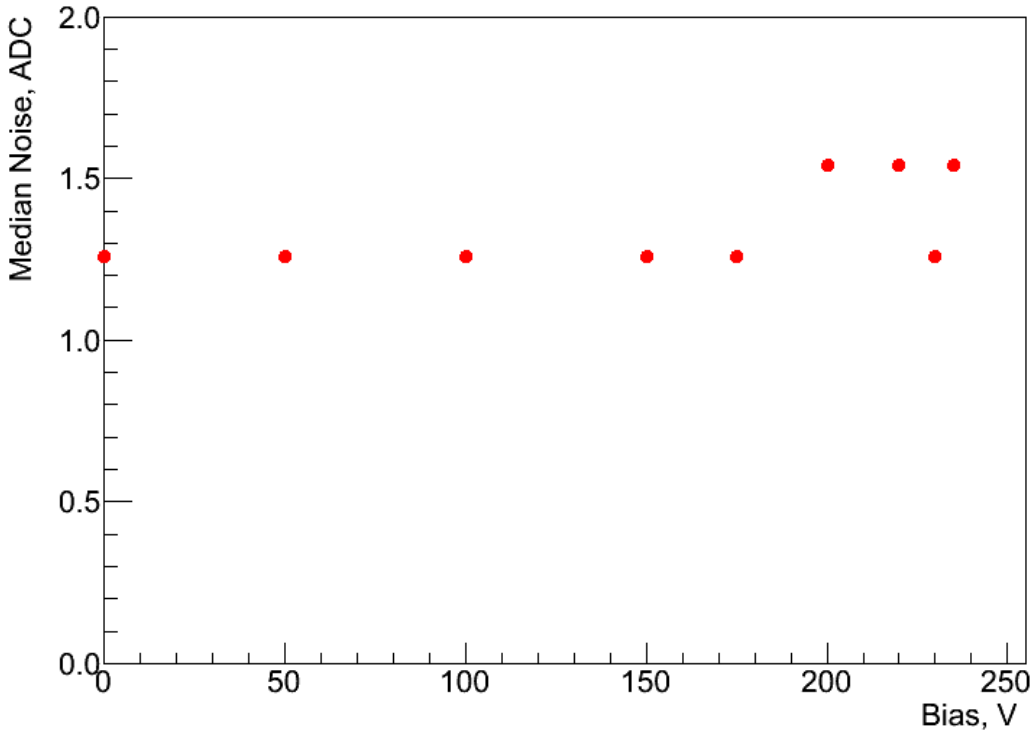

Figure 8. The noise as a function of bias voltage of 2×10^{15} n_{eq}/cm^2 irradiated $n^+/p^-/p^+$ CID detector.

The noise is 1.3 ADC up to 200V and then is followed by data points exhibiting higher noise values of about 1.6 ADC. In between the noisy runs above 200V, at 230V the noise is roughly 1.3 ADC. Thus, the S/N of this module is about 10.

Unlike the more heavily irradiated 5×10^{15} n_{eq}/cm^2 , the $n^+/p^-/p^+$ 2×10^{15} n_{eq}/cm^2 irradiated module could be measured also with reverse bias. The collected charge as a function of bias voltage for both reverse bias and CID operation modes is shown in figure 9.

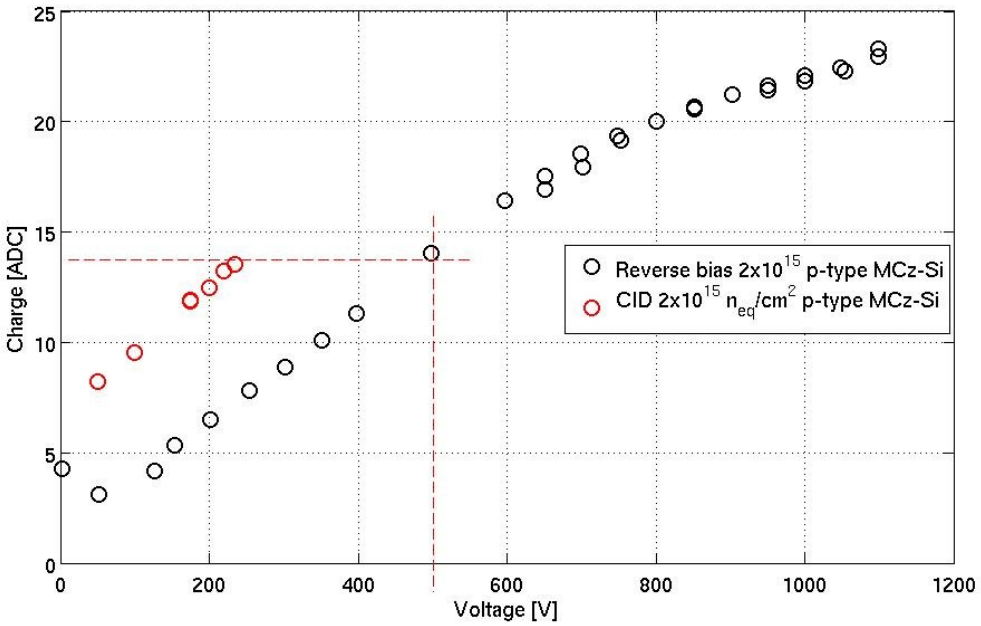

As it can be seen in figure 9., the 2×10^{15} n_{eq}/cm^2 irradiated module could be reverse biased up to 1100V. The leakage current at 1100V was about 14μA at -53^{0}C. The forward current at 200V was about 400μA. The same collected charge, 13.5 ADC at 230V, was obtained under reverse bias conditions at 500V as indicated in figure 9. The highest charge under reverse bias, at 1100V was about 24 ADC corresponding to about 60% relative CCE. Under 600V reverse bias, the 2×10^{15} n_{eq}/cm^2 irradiated $n^+/p^-/p^+$ MCz-Si module provides roughly the same CCE as similar $p^+/n^-/n^+$ MCz-Si detector irradiated with 1×10^{15} n_{eq}/cm^2 fluence reported in reference [1]. Comparison of the noise properties under reverse bias and CID mode is shown in figure 10.

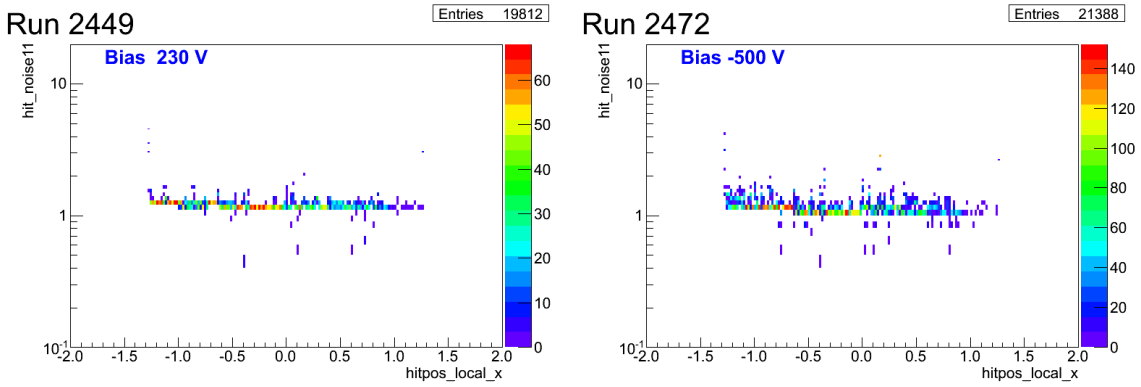

a) b)

Figure 10. Noise recorded from 2×10^{15} n_{eq}/cm^2 irradiated $n^+/p^-/p^+$ MCz-Si module a) CID mode at 230V and b) reverse bias 500V.

The average noise of the module when reverse biased at 500V is about 1.1 ADC. The collected charge is slightly less than 14 ADC, leading to S/N of about 12.5 .

3.Novel concept for 3D detectors based on electric field manipulation.

"Electric field manipulation" as an approach for the improvement of the radiation hardness of the silicon detectors that is the main subject of the RD39 collaboration currently, was extended on silicon detectors based on 3D technology. I.e. silicon detectors with collecting junctions penetrating partly or entirely through the bulk. The basic construction of the 3D detector presented in figure 11 has the narrow doped columns and the high resistivity silicon bulk. One type of columns form the P-N junctions and the others are the Ohmic contacts.

Under the reverse bias voltage applied between the junction columns and the Ohmic ones the electric field develops around the junction columns. The electric field distribution (as it follows from the Poisson equitation) is strongly non-uniform and has a maximum at the junction column surface (figure 11).

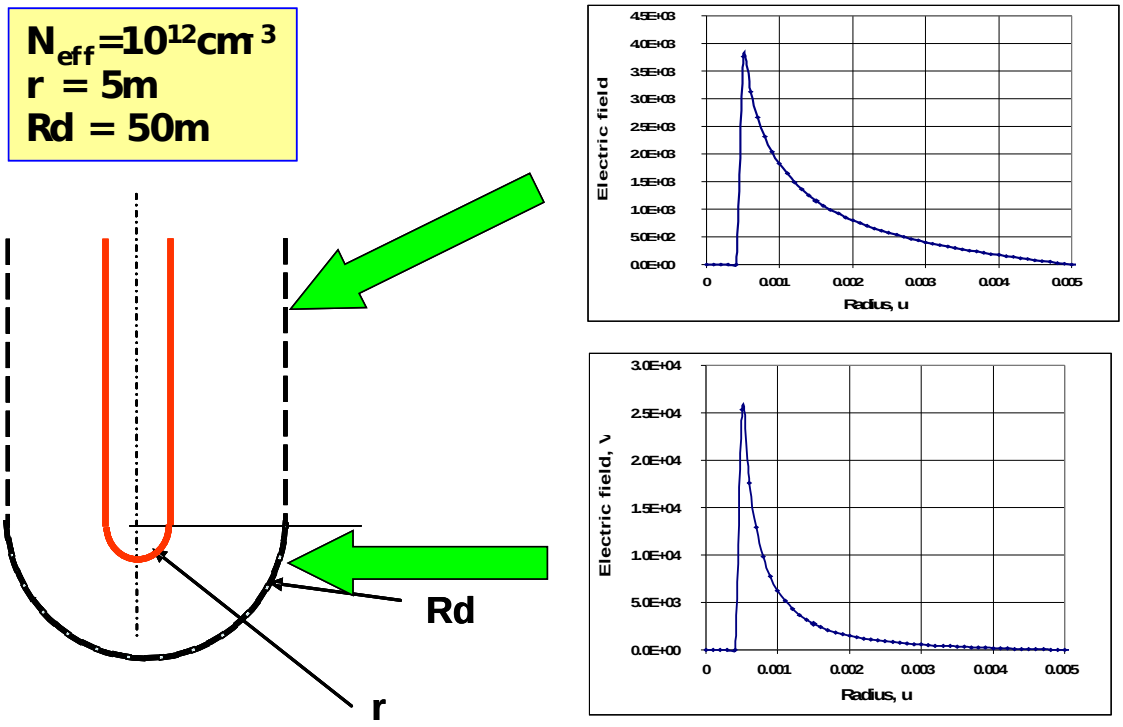

Figure 11. The electric focusing effect in 3D detectors

This focusing effect in a non-irradiated detector increases the maximum electric field up to 10^4 V/cm2 at tenth of volts applied to the detector. This value is far from the critical breakdown electric field which is an order of magnitude higher.

In the irradiated 3D detectors the electric field has the same focusing effect. However due to the effective concentration the geometrical focusing effect is magnified by a factor of 10 or more and becomes dangerous for the detector operation. The evaluation of the effect [9] predicts a breakdown at 300V for detectors irradiated to the fluence of 1×10^{16} n_{eq}/cm^2 . This voltage is lower than the value for the pinch off voltage i.e. the bias required to join the electric field regions of the neighboring junction columns, thus some parts of the detector volume will not be sensitive.

The new approach for an electric field manipulation in 3D detectors which is included in the plan of RD39, utilizes the effect of the junction electrode shape on the electric field. The physical idea is illustrated in figure 12.

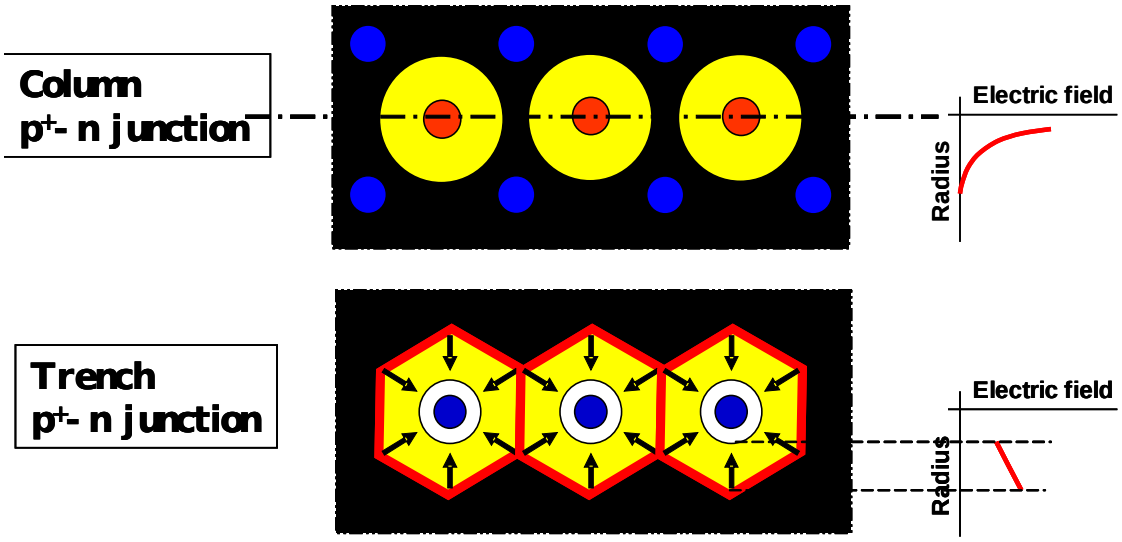

Figure 12. Schematic drawings of the "Junction column" – a and "Junction trench" 3D detectors and the electric field distributions in the sensitive volume (on the right).

The new structure is combined from the Ohmic column and the junction trench surrounding it. In this configuration the electric field is developed from the trench which is outer pert of the detecting cell towards the central Ohmic electrode. It is clear that in this configuration there is no electric field focusing effect until the cell is fully depleted. Even at over depletion the focusing effect at the Ohmic column will be damped by the space charge i.e. the sign of the gradient in the electric field due to the space charge and the focusing effect will be opposite. The result of solving the Poisson equation is presented in figure 13.

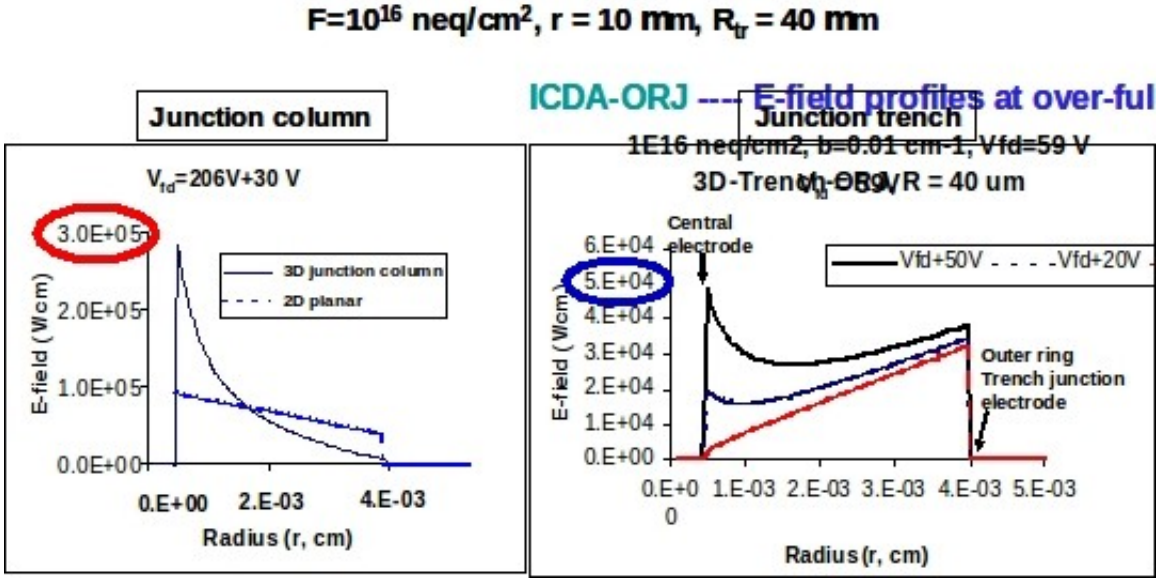

Figure 13 The electric field distribution in irradiated 3D detectors. A- Junction column type (compared with pad detector) and b- Junction trench type.

Even for the detector irradiated to the fluence of 1×10^{16} n_{eq}/cm^2 the electric field distribution does not have a sharp peak. Only at the over depletion the electric field exhibits the peak at the Ohmic column. However, the maximal electric field is low compared to the breakdown field.

The important feature which is specific for the junction trench configuration is the sufficiently low depletion voltage. The new configuration decreases the value from 200V to 59V, which is an important advantage for the application. The 3D junction trenched detectors are patented by Brookhaven National Laboratory (BNL), which is a member of the RD39 collaboration.

References

[1]1.P. Luukka, J. Härkönen, T. Mäenpää, B. Betchart, S. Bhattacharya, S. Czellar, R. Demina, A. Dierlamm, Y. Gotra, M. Frey, F. Hartmann, V. Karimäki, T. Keutgen, S. Korjenevski, M.J. Kortelainen, T. Lampén, V. Lemaitre, M. Maksimow, O. Militaru, H. Moilanen, Test beam results of heavily irradiated magnetic Czochralski silicon (MCz-Si) strip detectors, Nuclear Instruments and Methods in Physics Research A612 (2010) 497-500.
[2]G. Kramberger et al, Nucl. Instr. and Meth. **A481** (2002) 297.
[3]H.W. Kraner et al., Nucl. Instr. and Meth. A326 (1993) 350-356
[4]V. Eremin, J. Härkönen, P. Luukka, Z. Li, E. Verbitskaya, S. Väyrynen and I. Kassamakov, The operation and performance of Current Injected Detector (CID), Nuclear Instruments and Methods in Physics Research A581 (2007) 356-360.
[5]1.T. Mäenpää, P. Luukka, J. Härkönen et al.,Silicon beam telescope for LHC upgrade tests, Nuclear Instruments and Methods in Physics Research A593 (2008) 523-529.
[6]J. Härkönen, E. Tuovinen, P. Luukka, H.K. Nordlund and E. Tuominen, Magnetic Czochralski silicon as detector material, Nuclear Instruments and Methods in Physics Research A579 (2007) 648-652.
[7]RD39 Status Report 2008, CERN-LHCC-2008-019;LHCC-SR-001, http://cdsweb.cern.ch/record/1140477
[8]T.Mäenpää, M. Kotelainen and T. Lampen, Track-induced clustering in position sensitive detector characterization, IEEE Nuclear Science Symposium Conference Record (NSS/MIC), 2009, pages 832 – 835.
[9]V.Eremin, E.Verbitskaya, “Analytical approach for 3D detector engineering”, IEEE TNS